




Virial coefficients of hard hyperspherocylinders in \mathbb{R}^4 : Influence of the aspect ratio

Markus Kulossa , Philipp Marienhagen , and Joachim Wagner ^{*}
Institut für Chemie, Universität Rostock, 18051 Rostock, Germany

 (Received 25 February 2022; accepted 23 May 2022; published 21 June 2022)

We provide second- to sixth-order virial coefficients of hard hyperspherocylinders in dependence on their aspect ratio ν . Virial coefficients of an anisotropic geometry in four dimensions are calculated employing an optimized Mayer-sampling algorithm. As the second virial coefficient of a hard particle is identical to its excluded hypervolume, the numerically obtained second virial coefficients can be compared to analytical relations for the excluded hypervolume based on geometric measures of the respective, convex geometry in dependence on its aspect ratio ν .

DOI: [10.1103/PhysRevE.105.064121](https://doi.org/10.1103/PhysRevE.105.064121)

I. INTRODUCTION

Hard particles have been investigated thoroughly as a model for many-particle systems for more than a century. These studies have significantly contributed to the understanding of self-organization in condensed matter [1]. The virial series introduced by Kamerlingh Onnes [2],

$$p = \varrho k_B T (1 + B_2 \varrho + B_3 \varrho^2 + \dots), \quad (1)$$

where p denotes the pressure, $k_B T$ the thermal energy, and ϱ the particle number density, is the first attempt to describe thermodynamic properties of imperfect gases. The coefficients B_i in the MacLaurin expansion in number density accounting for the nonideal behavior are the virial coefficients. Introducing the volume fraction $\eta = \varrho V_P$ as the product of number density ϱ and particle volume V_P , with

$$p = \frac{\eta}{V_P} k_B T (1 + B_2^* \eta + B_3^* \eta^2 + \dots), \quad (2)$$

an expansion in terms of the volume fraction η results, where $B_i^* = B_i/V_P^{i-1}$ are reduced virial coefficients.

The first attempts to calculate virial coefficients use hard spheres as a model system with its geometric constraint of impenetrability [3–6]. The seminal work of Onsager with the analytically treatable model of infinitely thin rods predicted the formation of liquid-crystalline structures beyond a critical volume fraction [7]. Based on the theoretical foundation by means of statistical mechanics [8], with emerging computer performance, virial coefficients of order $5 \leq i \leq 12$ of hard spheres have been computed [9–15]. These methods have been extended to virial coefficients of anisometric hard bodies with different topology and aspect ratio [16–24].

Virial coefficients of hard discs as two-dimensional analogs of hard spheres have been theoretically [25,26] and numerically [27] calculated. For orders $i > 5$, in most cases, these virial coefficients were calculated together with those of hard spheres [10–12,28]. With these data, first insights into the

dimensionality's influence to the nonideal behavior of gases and supercritical fluids with impacts on the maximum packing fraction have been possible [29].

The extension of the hard-sphere model system to Euclidean spaces with dimensionality $D > 3$, already published by Ree and Hoover [30], does not only provide useful physical insights [31], but also has implications to information theory [32]. Virial coefficients of hard spheres in higher dimensions interestingly become negative for even orders i in dimensions $D \geq 5$ [33]. For hard hyperspheres, selected virial coefficients up to order $i = 64$ and up to dimension $D = 100$ are known [28]. Virial coefficients of anisometric, hard objects in dimensions $D > 3$, however, are so far unknown.

The aim of this contribution is the calculation of uniaxial, hard hyperspherocylinders' virial coefficients for dimension $D = 4$ in dependence on their aspect ratio ν . Since the second virial coefficient of hard, convex objects equals the mutual excluded volume, its relation to geometric measures is analyzed in dependence on the aspect ratio ν . Herewith, expressions for a four-dimensional analog of the Isihara-Hadwiger relation [34–36] can be tested.

II. THEORETICAL BACKGROUND

Using the Ree-Hoover reformulation, the virial coefficient of order i can be written as

$$B_i = -\frac{i-1}{i!} \sum_{G \in \mathcal{R}_i^L} c_G S_G, \quad (3)$$

where \mathcal{R}_i^L is the set of labeled Ree-Hoover graphs G with i vertices and weighting factors c_G , called Ree-Hoover star contents, depending on the graph's topology. S_G is the configuration integral over interactions represented by the labeled graph G . Since in the case of hard-body interaction a single Ree-Hoover diagram contributes to the integrand, the calculation based on the Mayer-sampling method [37] can be done employing an optimized algorithm with a bisection search in an ordered list containing all labeled diagrams with their star contents [23]. Mayer sampling as an importance sampling

^{*}joachim.wagner@uni-rostock.de

technique requires the simultaneous calculation of a known reference integral. For the calculation of the second virial coefficients the analytically known second virial coefficient of hard hyperspheres is used as a reference for small aspect ratios $\nu \leq 5$. To increase the accuracy for aspect ratios $\nu \geq 6$, as a reference, the virial coefficient of hard hyperspherocylinders with aspect ratio $\nu = 5$ obtained with hard hyperspheres as a reference is used. To minimize the total uncertainties for $\nu \geq 6$, this reference value is extensively sampled to reduce the uncertainty of this numerically obtained reference integral. For virial coefficients with order $i \geq 3$, however, integrals of highly branched spanning trees containing i vertices, each with the value $(-2B_2)^{i-1}$, are the more efficient choice as an intrinsic reference integral [23].

A. Geometric measures of hyperspherocylinders in \mathbb{R}^4

A hyperspherocylinder is the union of hyperspheres with radius r_{eq} the centers of which are located at $\mathbf{r} = \mathbf{c} + \lambda \hat{\mathbf{u}}$, where $\mathbf{c} = (c_w, c_x, c_y, c_z)^T$ is the hyperspherocylinder's center of mass and $\hat{\mathbf{u}} = (u_w, u_x, u_y, u_z)^T$ its direction indicated by a Cartesian unit vector. The parameter $-(\nu - 1)r_{\text{eq}} \leq \lambda \leq (\nu - 1)r_{\text{eq}}$ defines the length of the hypercylinder barrel and is related to the hyperspherocylinder's equatorial radius r_{eq} and its aspect ratio $\nu \geq 1$. The hypervolume V of a hyperspherocylinder with equatorial radius r_{eq} and aspect ratio ν reads as

$$V = \frac{16(\nu - 1) + 3\pi}{6} \pi r_{\text{eq}}^4, \quad (4)$$

and its hypersurface S can be written as

$$S = 2\pi[4(\nu - 1) + \pi]r_{\text{eq}}^3. \quad (5)$$

Its mean radius of curvature \tilde{R} is accessible as the hypersurface integral of its mean curvature κ [38,39]. Since the latter quantity is $\kappa = 1/(3r_{\text{eq}}^2)$ in the hypercylindrical part with length $2(\nu - 1)r_{\text{eq}}$, $1/r_{\text{eq}}^2$ in both hemihyperspheres, and the curvature is continuous at the entire hypersurface, a hyperspherocylinder's mean radius of curvature \tilde{R} reads as

$$\tilde{R} = \left[\frac{4(\nu - 1)}{3\pi} + 1 \right] r_{\text{eq}}. \quad (6)$$

B. Overlap criteria for hyperspherocylinders

Let \mathbf{c}_1 and \mathbf{c}_2 be two hyperspherocylinders' centers of mass, $\hat{\mathbf{u}}_1$ and $\hat{\mathbf{u}}_2$ unit vectors describing their orientation, r_{eq} their equatorial radius, and ν their aspect ratio. The overlap problem of hard hyperspherocylinders in \mathbb{R}^4 can be solved by determination of the minimum distance between the two lines $\mathbf{r}_1(\lambda) = \mathbf{c}_1 + \lambda \hat{\mathbf{u}}_1$ and $\mathbf{r}_2(\mu) = \mathbf{c}_2 + \mu \hat{\mathbf{u}}_2$ under the constraints $|\lambda| \leq (\nu - 1)r_{\text{eq}}$ and $|\mu| \leq (\nu - 1)r_{\text{eq}}$ in analogy to the overlap problem in \mathbb{R}^3 [40]. If the minimum distance is $|\mathbf{r}_1(\lambda_{\text{min}}) - \mathbf{r}_2(\mu_{\text{min}})| \leq 2r_{\text{eq}}$, both hyperspherocylinders overlap, otherwise not. This overlap criterion can easily be extended to arbitrary dimensions D .

C. Simulation details

The calculation of the i th virial coefficient of an uniaxial solid of revolution in \mathbb{R}^4 requires an integration over a $7(i - 1)$ -dimensional configuration space which can be per-

formed efficiently using a Mayer-sampling algorithm [37] extended to the four-dimensional space. In the case of hard-body systems, the originally proposed acceptance criterion has to be adapted by using a weighted sum of the integrands of both the system of interest and the reference system [23]. The algorithm is based on random translation and rotation attempts of randomly selected particles.

Let $\Omega = (\vartheta, \chi, \varphi)$ be the angular coordinates of a random unit vector in \mathbb{R}^4 with the probability densities $p(\vartheta) = 2 \sin^2 \vartheta / \pi$, $p(\chi) = \sin \chi / 2$, and $p(\varphi) = 1/(2\pi)$ in $0 \leq \vartheta \leq \pi$, $0 \leq \chi \leq \pi$, and $0 \leq \varphi \leq 2\pi$. With the abbreviations $a = \cos \vartheta$, $b = \sin \vartheta \cos \chi$, $c = \sin \vartheta \sin \chi \sin \varphi$, and $d = \sin \vartheta \sin \chi \cos \varphi$, a randomly oriented unit vector $\hat{\mathbf{u}} = (-d, -c, -b, a)^T$ is generated. A random translation of a particle is achieved by choosing its center-of-mass position \mathbf{c}_{N+1} at step $N + 1$ relative to its previous position \mathbf{c}_N :

$$\mathbf{c}_{N+1} = \mathbf{c}_N + \Delta_{\text{trans}} \xi \hat{\mathbf{u}}, \quad (7)$$

where $0 \leq \xi \leq 1$ is a uniformly distributed random number. The maximum length of displacement Δ_{trans} is tuned to obtain an acceptance ratio of $p_{\text{acc}} \approx 1/2$.

Using again random angular coordinates Ω , a left isoclinic rotation matrix in \mathbb{R}^4 can be written as

$$\mathbf{R}(\Omega) = \begin{pmatrix} a & -b & c & -d \\ b & a & -d & -c \\ -c & d & a & -b \\ d & c & b & a \end{pmatrix} \quad (8)$$

based on the Hamilton quaternion [41]. Additionally employing a rotation matrix

$$\Psi(\psi) = \mathbf{R}(\psi, 0, 0)$$

$$= \begin{pmatrix} \cos \psi & -\sin \psi & 0 & 0 \\ \sin \psi & \cos \psi & 0 & 0 \\ 0 & 0 & \cos \psi & -\sin \psi \\ 0 & 0 & \sin \psi & \cos \psi \end{pmatrix}, \quad (9)$$

a randomly rotated unit vector $\hat{\mathbf{u}}_{N+1}$ can be obtained from the orientation of a given particle $\hat{\mathbf{u}}_N$ at step N by

$$\hat{\mathbf{u}}_{N+1} = \mathbf{R}(\Omega) \cdot \Psi(\psi) \cdot \mathbf{R}^T(\Omega) \cdot \hat{\mathbf{u}}_N. \quad (10)$$

Choosing ψ with $-\Delta_{\text{rot}} \leq \psi \leq \Delta_{\text{rot}}$ as a random number with probability density $p(\psi) = 1/(2\Delta_{\text{rot}})$ allows an exploration of the rotational configuration space with uniform density at the unit hypersphere's hypersurface as shown in the Appendix complemented by a detailed description of the rotation. The maximum rotation Δ_{rot} is again chosen to obtain an acceptance probability of $p_{\text{acc}} \approx 1/2$.

The calculation of virial coefficients with known overlaps and nonoverlaps is independent of the systems' dimensionality and thus identical to the strategy in \mathbb{R}^2 and \mathbb{R}^3 as described in [23]: After translation and rotation of a selected particle $i(i - 1)/2$ Mayer f functions f_{jk} are calculated based on overlaps and nonoverlaps between particles j and k of the obtained configuration, where, in the case of an overlap between particles j and k , $f_{jk} = -1$ is obtained and otherwise $f_{jk} = 0$ results. Defining additionally $e_{jk} = f_{jk} + 1$, the contribution of the generated configuration to the virial coefficient [Eq. (3)] is a product of f and e functions of the single contributing graph G weighted by its star content c_G [10].

TABLE I. Reduced virial coefficient B_i^* of hard, four-dimensional hyperspherocylinders with the aspect ratio ν .

ν	B_2^*	B_3^*	B_4^*	B_5^*	B_6^*
1		32.4061 (19)	77.743 (9)	146.23 (6)	253.2 (8)
	8	32.405759... ^a	77.745183... ^a	146.2451 (5) ^a	253.388 (6) ^a
2	9.6026 (4)	42.7361 (20)	96.325 (14)	174.58 (16)	340 (4)
3	11.9340 (6)	57.9720 (29)	108.70 (4)	270.5 (5)	444 (19)
4	14.3853 (7)	74.454 (9)	104.28 (5)	564.3 (13)	-850 (40)
5	16.87831 (21)	91.606 (11)	81.18 (7)	1213.2 (22)	-7000 (130)
6	19.3904 (11)	109.188 (21)	39.09 (14)	2363 (7)	-23500 (400)
7	21.9132 (13)	127.076 (25)	-21.31 (16)	4161 (12)	-57500 (600)
8	24.4416 (16)	145.19 (4)	-99.59 (24)	6723 (27)	-119000 (1100)
9	26.9744 (11)	163.52 (5)	-194.71 (24)	10180 (40)	-215600 (1900)
10	29.5108 (17)	182.00 (9)	-306.7 (6)	14581 (30)	-360000 (4000)

^aValue from [28].

For the calculation of virial coefficients of order 2–6 at least 16 independent runs, each with 5×10^{10} Monte Carlo steps, are used. The data provided are averages with confidence intervals given by standard errors.

III. RESULTS AND DISCUSSION

The calculated virial coefficients of hard hyperspherocylinders with aspect ratios $1 \leq \nu \leq 10$ from order 2–6 are compiled in Table I. The literature values for hard hyperspheres' virial coefficients are in the limit $\nu \rightarrow 1^+$ reproduced within their uncertainties for the orders $3 \leq i \leq 6$. Since the scope of this paper is an aspect-ratio dependent approach covering orientation averages of anisotropic particles, the numerical effort is drastically increased. The larger uncertainties compared to hard hyperspheres' virial coefficients in [28] are therefore not a principal limitation of the used algorithm, but a consequence of the significantly enlarged computational demands.

A. Second virial coefficient and excluded hypervolume

Using the geometric measures of hypersurface S , mean radius of curvature \tilde{R} , and particle hypervolume V_p , the relation

$$B_2^* = 1 + \frac{7 S \tilde{R}}{4 V_p} \quad (11)$$

was proposed for convex geometries as the excluded hypervolume per particle in \mathbb{R}^4 [38], which is in the case of hard-body interaction identical to the second virial coefficient. While this relation is valid for a hypersphere in the limit $\nu \rightarrow 1^+$, for larger aspect ratios severe discrepancies to second virial coefficients calculated by means of Mayer sampling arise (Fig. 1). However, the relation

$$B_2^* = 2 \frac{S \tilde{R}}{V_p} = \frac{8}{\pi} \frac{[4(\nu - 1) + 3\pi][4(\nu - 1) + \pi]}{16(\nu - 1) + 3\pi} \quad (12)$$

describes the reduced second virial coefficients for $1 \leq \nu \leq 10$ with high accuracy.

Recently, the same authors corrected their conjecture (11) using mixed volumes and quermassintegrals [42]. For a convex set K , the excluded hypervolume per particle v_{ex} and thus the second virial coefficient can in the four-dimensional space

be written as

$$B_2 = v_{\text{ex}} = \frac{1}{2\kappa_4} \sum_{i=0}^4 \binom{4}{i} W_i(K) W_{4-i}(K), \quad (13)$$

where $\kappa_4 = \pi^2/2$ is the hypervolume of the unit hypersphere in \mathbb{R}^4 and $W_i(K)$ are quermassintegrals of K . With the latter quantities, B_2 can be written as

$$B_2 = \frac{2}{\pi^2} [W_0(K)W_4(K) + 4W_1(K)W_3(K) + 3W_2^2(K)]. \quad (14)$$

$W_0(K) = V_p^{(D)}(K)$ is the D -dimensional hypervolume of a convex shape, $W_1(K) = S^{(D-1)}(K)/D$ its $(D-1)$ -dimensional hypersurface, $W_{D-1}(K) = \kappa_D \tilde{R}$ its mean radius of curvature \tilde{R} multiplied by the hypervolume κ_D of a D -dimensional unit

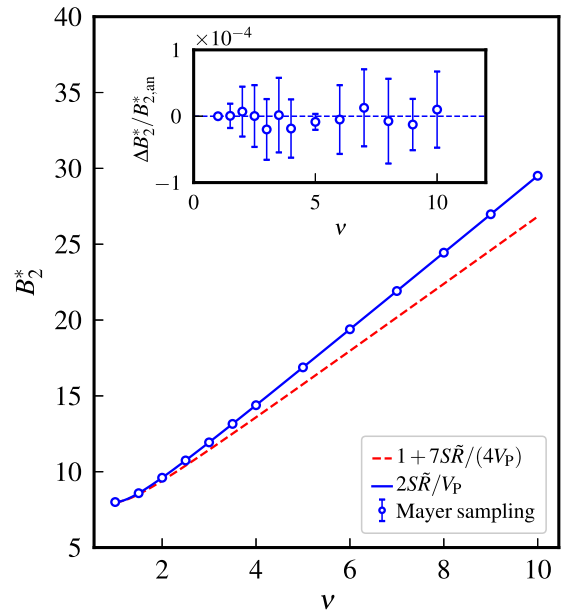


FIG. 1. Reduced second virial coefficients $B_2^* = B_2/V_p$ for hard, four-dimensional hyperspherocylinders in dependence on the aspect ratio ν . The dashed red line represents relation Eq. (11), while the blue solid line represents Eq. (12). The inset displays the relative deviations $\Delta B_2^* = B_2^* - B_{2,\text{an}}^*$ between numerically calculated, reduced second virial coefficients B_2^* and analytically calculated $B_{2,\text{an}}^*$ employing Eq. (12).

hypersphere, and finally $W_D(\mathbf{K}) = \kappa_D$ the hypervolume of the D -dimensional unit hypersphere. Using these quantities, B_2 of a convex shape in \mathbb{R}^4 can be expressed as

$$B_2 = V_p^{(4)}(\mathbf{K}) + S^{(3)}(\mathbf{K})\tilde{R}(\mathbf{K}) + \frac{6}{\pi^2}W_2^2(\mathbf{K}) \quad (15)$$

with the missing quermassintegral

$$W_2 = \frac{\pi^2}{2}r_{\text{eq}}^2 + \frac{4\pi}{3}(\nu - 1)r_{\text{eq}}^2 \quad (16)$$

of a hyperspherocylinder in \mathbb{R}^4 [43,44]. As easily can be seen, this leads to $V_p + 6W_2^2/\pi^2 = S\tilde{R}$ and results in the analytical expression $B_2 = 2S\tilde{R}$ and therewith $B_2^* = 2S\tilde{R}/V_p$. The relation $V_p + 6W_2^2/\pi^2 = S\tilde{R}$ is to our knowledge unique for hyperspherocylinders in \mathbb{R}^4 .

In the limit of infinitely long hyperspherocylinders, Eq. (12) leads to

$$\lim_{\nu \rightarrow \infty} \frac{B_2^*(\nu)}{\nu} = \frac{8}{\pi} \quad (17)$$

indicating an excluded hypervolume proportional to the aspect ratio ν .

In the two-dimensional Euclidean space with the figure's area A_F , the circumference S , and the mean radius of curvature $\tilde{R} = S/(2\pi)$, the reduced second virial coefficient can be written as $B_2^* = 1 + S\tilde{R}/(2A_F) = 1 + S^2/(4\pi A_F)$ [45]. In the three-dimensional Euclidean space, the relation $B_2^* = 1 + S\tilde{R}/V_p$ is obtained with the surface S , the mean radius of curvature \tilde{R} , and the particle volume V_p [34–36].

Despite that the hypervolume in Eq. (12) is not an additive contribution to the excluded hypervolume, the formulation based on quermassintegrals [Eq. (15)] shows that the hypervolume in fact contributes to the mutual excluded hypervolume. In analogy to the excluded volume in the two- and three-dimensional space, also in four- and higher-dimensional Euclidean spaces, the D -dimensional hypervolumes are additive contributions to the mutual excluded hypervolume.

B. Higher-order virial coefficients

The excellent agreement of our numerical results for the second virial coefficients with the analytical result [Eq. (12)] proves the correctness of the Mayer-sampling algorithm and the overlap criterion in \mathbb{R}^4 . The third- to sixth-order virial coefficients in Table I are calculated using this analytical result as an exact reference integral. Noticeably, the higher-order virial coefficients exhibit alternating signs between even and odd orders at large aspect ratios: The even-order virial coefficients B_4^* and B_6^* are negative and strongly decrease with increasing aspect ratio ν , while the odd-order virial coefficients B_3^* and B_5^* are positive and notably increase with the aspect ratio ν . This behavior is also known for hyperspheres in dimensions $D \geq 8$ for third- and higher-order virial coefficients [28].

For convex figures in two dimensions and for oblate geometries in three dimensions, a nearly linear dependence of reduced virial coefficients $\tilde{B}_i = B_i/B_2^{i-1}$ on the inverse excess part of the excluded volume α appears especially for lower-order virial coefficients [23,46]. Employing Eq. (12), in four dimensions $\alpha = (B_2 - V_p)/(7V_p) = (2S\tilde{R}/V_p - 1)/7$ results,

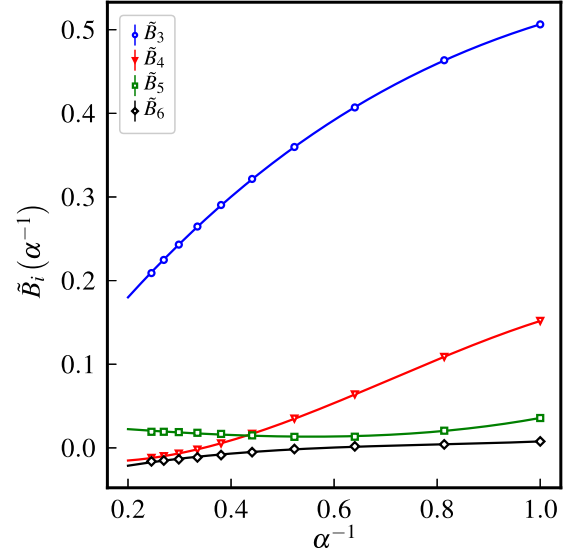


FIG. 2. Reduced virial coefficients $\tilde{B}_i = B_i/B_2^{i-1}$ in dependence on the inverse of the rescaled, excess part $\alpha = (2S\tilde{R}/V_p - 1)/7$ of the excluded hypervolume. The solid lines are least-squares fits employing a third-order polynomial as a heuristic approach.

where the scaling factor $1/7$ guarantees $\alpha(\nu \rightarrow 1^+) = 1$ in the limit of a hypersphere.

In the case of four-dimensional hyperspherocylinders, consistent with results for three-dimensional spherocylinders [47], already for the third-order reduced virial coefficient \tilde{B}_3 , a significant nonlinearity is observed (Fig. 2). However, the reduced virial coefficients \tilde{B}_i of order 3–6 can excellently be described using a third-order polynomial in dependence on the aspect ratio ν and therewith reliably be interpolated.

IV. OUTLOOK

With the described approach, for the first time virial coefficients of four-dimensional, anisotropic objects are calculated. Using hard hyperspherocylinders exemplarily as a convex shape with tunable aspect ratio ν in \mathbb{R}^4 , the impact of anisometry to the geometric measures of hypervolume, hypersurface, mean radius of curvature, and the quermassintegral W_2 can be analyzed and related to the second virial coefficient.

Our numerical results for B_2 agree with the analytical result employing mixed volumes and quermassintegrals [42]. A remaining task is the calculation of virial coefficients with order $i > 6$ for four-dimensional hyperspherocylinders and virial coefficients of differently shaped, hard anisotropic objects in \mathbb{R}^4 .

ACKNOWLEDGMENTS

P.M. gratefully acknowledges financial support by the Universität Rostock within the Ph.D. scholarship program.

APPENDIX: EXPLORATION OF THE ROTATIONAL CONFIGURATION SPACE

Let $\Omega_N = (\vartheta_N, \chi_N, \varphi_N)$ be generalized angular coordinates describing the orientation of an uniaxial solid of revolution in

\mathbb{R}^4 at step N . The orientation alternatively can be written as

$$\hat{\mathbf{u}}_N = \begin{pmatrix} \sin \vartheta_N \sin \chi_N \cos \varphi_N \\ \sin \vartheta_N \sin \chi_N \sin \varphi_N \\ \sin \vartheta_N \cos \chi_N \\ \cos \vartheta_N \end{pmatrix} \quad (\text{A1})$$

using the Cartesian unit vector $\hat{\mathbf{u}}_N$. A random rotation in \mathbb{R}^4 can be achieved as follows.

(i) Generate a randomly oriented unit vector $\hat{\mathbf{u}}_r$. Let $0 \leq \vartheta_r \leq \pi$ be a random number with probability density $p(\vartheta_r) = 2 \sin^2 \vartheta_r / \pi$, $0 \leq \chi_r \leq \pi$ a random number with probability density $p(\chi_r) = \sin \chi_r / 2$, and $0 \leq \varphi_r \leq 2\pi$ a random number with probability density $p(\varphi) = 1/(2\pi)$.

Using the definitions

$$d = \sin \vartheta_r \sin \chi_r \cos \varphi_r, \quad (\text{A2a})$$

$$c = \sin \vartheta_r \sin \chi_r \sin \varphi_r, \quad (\text{A2b})$$

$$b = \sin \vartheta_r \cos \chi_r, \quad (\text{A2c})$$

$$a = \cos \vartheta_r, \quad (\text{A2d})$$

a left isoclinic rotation matrix in \mathbb{R}^4 [41] can be written as

$$\mathbf{R}(\boldsymbol{\Omega}_r) = \begin{pmatrix} a & -b & c & -d \\ b & a & -d & -c \\ -c & d & a & -b \\ d & c & b & a \end{pmatrix} \quad (\text{A3})$$

with the generalized angular coordinates $\boldsymbol{\Omega}_r = (\vartheta_r, \chi_r, \varphi_r)$ and the corresponding unit vector $\hat{\mathbf{u}}_r = (-d, -c, -b, a)^T$. Using $\mathbf{R}^T(\boldsymbol{\Omega}_r) \cdot \hat{\mathbf{u}}_r$, the random unit vector $\hat{\mathbf{u}}_r$ is rotated, resulting in a unit vector in the positive z direction $\hat{\mathbf{u}}_z = (0, 0, 0, 1)^T$.

(ii) Using an additional rotation matrix

$$\boldsymbol{\Psi}(\psi) = \mathbf{R}(\psi, 0, 0)$$

$$= \begin{pmatrix} \cos \psi & -\sin \psi & 0 & 0 \\ \sin \psi & \cos \psi & 0 & 0 \\ 0 & 0 & \cos \psi & -\sin \psi \\ 0 & 0 & \sin \psi & \cos \psi \end{pmatrix}, \quad (\text{A4})$$

describing a counterclockwise rotation by ψ , the unit vector $\hat{\mathbf{u}}_\psi = (0, 0, -\sin \psi, \cos \psi)^T$ results from

$$\hat{\mathbf{u}}_\psi = (0, 0, -\sin \psi, \cos \psi)^T = \boldsymbol{\Psi}(\psi) \cdot \hat{\mathbf{u}}_z. \quad (\text{A5})$$

(iii) Applying

$$\hat{\mathbf{u}}_{\psi, \boldsymbol{\Omega}_r} = \mathbf{R}(\boldsymbol{\Omega}_r) \cdot \hat{\mathbf{u}}_\psi, \quad (\text{A6})$$

the intermediate result $\hat{\mathbf{u}}_\psi$ is back-transformed to the initial coordinate system. Combining (i)–(iii)

$$\boldsymbol{\Xi}(\boldsymbol{\Omega}_r, \psi) = \mathbf{R}(\boldsymbol{\Omega}_r) \cdot \boldsymbol{\Psi}(\psi) \cdot \mathbf{R}^T(\boldsymbol{\Omega}_r) \quad (\text{A7})$$

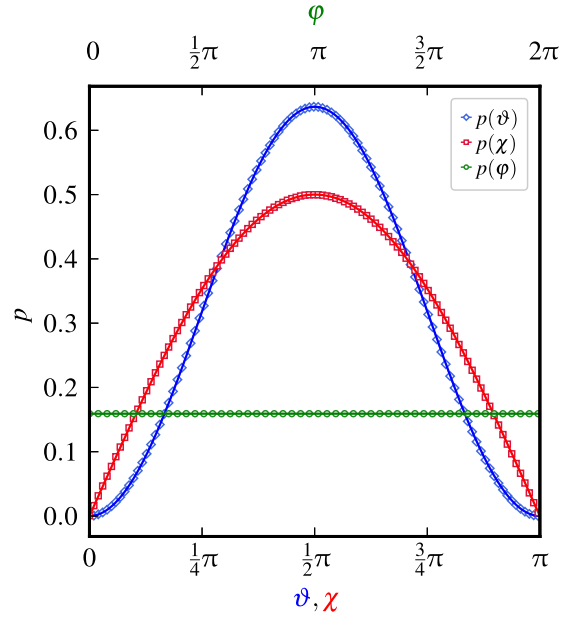


FIG. 3. Probability densities of polar angles ϑ , χ , and φ obtained during 10^{10} random rotations according to Eq. (A8) with $\Delta_{\text{rot}} = 1/2$ starting from the initial orientation $\hat{\mathbf{u}}_1 = (0, 0, 0, 1)^T$. The solid lines represent the theoretically expected probability densities.

results, which again is a rotation matrix in \mathbb{R}^4 with the properties $\boldsymbol{\Xi}^T(\boldsymbol{\Omega}_r, \psi) \cdot \boldsymbol{\Xi}(\boldsymbol{\Omega}_r, \psi) = \mathbf{I}$ and $\det(\boldsymbol{\Xi}(\boldsymbol{\Omega}_r, \psi)) = 1$, where \mathbf{I} denotes the identity. Choosing a random orientation vector $\boldsymbol{\Omega}_r$ and a random number $-\Delta_{\text{rot}} \leq \psi \leq \Delta_{\text{rot}}$ with probability density $p(\psi) = 1/(2\Delta_{\text{rot}})$, a consecutive application of $\boldsymbol{\Xi}(\boldsymbol{\Omega}_r, \psi)$

$$\hat{\mathbf{u}}_{N+1} = \boldsymbol{\Xi}(\boldsymbol{\Omega}_r, \psi) \cdot \hat{\mathbf{u}}_N \quad (\text{A8})$$

to a particles' orientation $\hat{\mathbf{u}}_N$ at step N leads to a homogeneous exploration of a unit hypersphere's hypersurface as shown in Fig. 3. The probability densities are obtained during 10^{10} random rotations employing Eq. (A8) using $\Delta_{\text{rot}} = 1/2$ and starting from the initial orientation $\hat{\mathbf{u}}_1 = (0, 0, 0, 1)^T$. The solid lines are the theoretical probability densities $p(\vartheta) = 2 \sin^2 \vartheta / \pi$, $p(\chi) = \sin \chi / 2$, and $p(\varphi) = 1/(2\pi)$. The excellent agreement of the obtained probability densities with the theoretical predictions proves a homogeneous exploration of the rotational configuration space by the described method.

- [1] S. Torquato, *J. Chem. Phys.* **149**, 020901 (2018).
 [2] H. Kamerlingh Onnes, *Proc. K. Ned. Akad. Wet.* **4**, 125 (1902).
 [3] B. Jäger, *Sitzungsber. Akad. Wiss. Wien, Math.-Naturwiss. Kl., Abt. 2A* **105**, 15 (1896).
 [4] J. D. van der Waals, *Proc. K. Ned. Akad. Wet.* **1**, 138 (1899).
 [5] L. Boltzmann, *Sitzungsber. Akad. Wiss. Wien, Math.-Naturwiss. Kl., Abt. 2A* **105**, 695 (1896).

- [6] L. Boltzmann, *Proc. K. Ned. Akad. Wet.* **1**, 398 (1899).
 [7] L. Onsager, *Ann. NY Acad. Sci.* **51**, 627 (1949).
 [8] J. E. Mayer and M. G. Mayer, *Statistical Mechanics* (Wiley, New York, 1940).
 [9] M. N. Rosenbluth and A. W. Rosenbluth, *J. Chem. Phys.* **22**, 881 (1954).
 [10] F. H. Ree and W. G. Hoover, *J. Chem. Phys.* **40**, 939 (1964).

- [11] F. H. Ree and W. G. Hoover, *J. Chem. Phys.* **46**, 4181 (1967).
- [12] E. J. Janse van Rensburg, *J. Phys. A: Math. Gen.* **26**, 4805 (1993).
- [13] S. Labík, J. Kolafa, and A. Malijeviský, *Phys. Rev. E* **71**, 021105 (2005).
- [14] R. J. Wheatley, *Phys. Rev. Lett.* **110**, 200601 (2013).
- [15] A. J. Schultz and D. A. Kofke, *Phys. Rev. E* **90**, 023301 (2014).
- [16] P. A. Monson and M. Rigby, *Mol. Phys.* **35**, 1337 (1978).
- [17] D. Frenkel, *J. Phys. Chem.* **91**, 4912 (1987).
- [18] M. Rigby, *Mol. Phys.* **66**, 1261 (1989).
- [19] W. R. Cooney, S. M. Thompson, and K. E. Gubbins, *Mol. Phys.* **66**, 1269 (1989).
- [20] J. A. C. Veerman and D. Frenkel, *Phys. Rev. A* **45**, 5632 (1992).
- [21] C. Vega, *Mol. Phys.* **92**, 651 (1997).
- [22] A. Y. Vlasov, X.-M. You, and A. J. Masters, *Mol. Phys.* **100**, 3313 (2002).
- [23] P. Marienhagen, R. Hellmann, and J. Wagner, *Phys. Rev. E* **104**, 015308 (2021).
- [24] P. Marienhagen and J. Wagner, *Phys. Rev. E* **105**, 014125 (2022).
- [25] L. Tonks, *Phys. Rev.* **50**, 955 (1936).
- [26] P. C. Hemmer, *J. Chem. Phys.* **42**, 1116 (1965).
- [27] N. Metropolis, A. W. Rosenbluth, M. N. Rosenbluth, A. H. Teller, and E. Teller, *J. Chem. Phys.* **21**, 1087 (1953).
- [28] C. Zhang and B. M. Pettitt, *Mol. Phys.* **112**, 1427 (2014).
- [29] M. Á. G. Maestre, A. Santos, M. Robles, and M. L. de Haro, *J. Chem. Phys.* **134**, 084502 (2011).
- [30] F. H. Ree and W. G. Hoover, *J. Chem. Phys.* **40**, 2048 (1964).
- [31] M. Adda-Bedia, E. Katzav, and D. Vella, *J. Chem. Phys.* **129**, 144506 (2008).
- [32] J. H. Conway and N. J. A. Sloane, *Sphere Packings, Lattices and Groups*, Vol. 290 (Springer, New York, 2013).
- [33] N. Clisby and B. M. McCoy, *J. Stat. Phys.* **122**, 15 (2006).
- [34] A. Isihara, *J. Chem. Phys.* **18**, 1446 (1950).
- [35] A. Isihara and T. Hayashida, *J. Phys. Soc. Jpn.* **6**, 40 (1951).
- [36] H. Hadwiger, *Experientia* **7**, 395 (1951).
- [37] J. K. Singh and D. A. Kofke, *Phys. Rev. Lett.* **92**, 220601 (2004).
- [38] S. Torquato and Y. Jiao, *Phys. Rev. E* **87**, 022111 (2013).
- [39] E. Herold, R. Hellmann, and J. Wagner, *J. Chem. Phys.* **147**, 204102 (2017).
- [40] C. Vega and S. Lago, *Comput. Chem.* **18**, 55 (1994).
- [41] A. Perez-Gracia and F. Thomas, *Adv. Appl. Clifford Algebras* **27**, 523 (2017).
- [42] S. Torquato and Y. Jiao, [arXiv:2203.16764](https://arxiv.org/abs/2203.16764).
- [43] R. Schneider, *Convex Bodies: The Brunn-Minkowski Theory*, Vol. 151 (Cambridge University Press, Cambridge, 2014).
- [44] L. A. Santaló, *Integral Geometry and Geometric Probability* (Cambridge University Press, Cambridge, 2004).
- [45] T. Boublík, *Mol. Phys.* **27**, 1415 (1974).
- [46] M. Rigby, *Mol. Phys.* **78**, 21 (1993).
- [47] M. Francová, J. Kolafa, P. Morávek, S. Labík, and A. Malijeviský, *Collect. Czech. Chem. Commun.* **73**, 413 (2008).